Journal of Cellular Biochemistry 90:109–120 (2003)

Fluorescence Activated Cell Sorting Reveals Heterogeneous and Cell Non-Autonomous Osteoprogenitor Differentiation in Fetal Rat Calvaria Cell Populations

Kelly A. Purpura,[1,2] Peter W. Zandstra,[1,2] and Jane E. Aubin[2,3]*

[1]Department of Chemical Engineering and Applied Chemistry, University of Toronto, Toronto, Ontario, Canada
[2]Institute of Biomaterials and Biomedical Engineering, University of Toronto, Toronto, Ontario, Canada
[3]Department of Molecular and Medical Genetics, University of Toronto, Toronto, Ontario, Canada

Abstract Identification of osteoblast progenitors, with defined developmental capacity, would facilitate studies on a variety of parameters of bone development. We used expression of alkaline phosphatase (ALP) and the parathyroid hormone/parathyroid hormone-related protein receptor (PTH1R) as osteoblast markers in dual-color fluorescence activated cell sorting (FACS) to fractionate rat calvaria (RC) cells into ALP^-PTH1R^-, ALP^+PTH1R^-, ALP^-PTH1R^+, and ALP^+PTH1R^+ populations. These fractionated populations were seeded clonally ($n = 96$) or over a range of cell densities ($\sim$150–8,500 cell/cm^2; $n = 3$). Our results indicate that colony forming unit-osteoblast (CFU-O)/bone nodule-forming cells are found in all fractions, but the frequency of CFU-O and total mineralized area is different across fractions. Analysis of these differences suggests that ALP^-PTH1R^-, ALP^-PTH1R^+, ALP^+PTH1R^-, and ALP^+PTH1R^+ cell populations are separated in order of increasing bone formation capacity. Dexamethasone (dex) differentially increased the CFU-O number in the four fractions, with the largest stimulation in the ALP^- cell populations. However, there was no significant difference in the number or size distribution of CFU-F (fibroblast) colonies that formed in vehicle versus dex. Finally, both cell autonomous and cell non-autonomous (i.e., inhibitory/stimulatory effects of cell neighbors) differentiation of osteoprogenitors was seen. Only the ALP^-PTH1R^- population was capable of forming nodules at the clonal level, at approximately 3- or 12-times the predicted frequency of unfractionated populations in dex or vehicle, respectively. These data suggest that osteoprogenitors can be significantly enriched by fractionation of RC populations, that assay conditions modify the osteoprogenitor frequencies observed and that fractionation of osteogenic populations is useful for interrogation of their developmental status and osteogenic capacity. J. Cell. Biochem. 90: 109–120, 2003.

Key words: osteoprogenitors; hierarchy; alkaline phosphatase; parathyroid hormone/parathyroid hormone-related protein receptor; colony forming unit-osteoblast

In primary bone- or bone marrow (BM)-derived cell cultures of a variety of species (e.g., chicken, human, mouse, rat), a subpopulation of cells is capable of forming three-dimensional nodules resembling woven bone [Bellows et al., 1986; Gerstenfeld et al., 1987; Falla et al., 1993; Bellows et al., 1998; Nishida et al., 1999; Siggelkow et al., 1999]. These nodules are the endpoint of a proliferation–differentiation sequence of osteoprogenitors and serve as the basis of the colony forming unit-osteoblast (CFU-O) assay. In the rat calvaria (RC) model used in this study, limiting dilution analysis has suggested that approximately 0.3% of the RC population is a CFU-O under standard culture conditions and that only one cell type is limiting, suggested to be the osteoprogenitors themselves [Bellows and Aubin, 1989].

Grant sponsor: CIHR (Operating Grants, to JEA); Grant number: MT-12390; Grant sponsor: PREA (to PWZ); Grant sponsor: Stem Cell Network (to JEA, PWZ); Grant sponsor: NSERC (to PWZ).

*Correspondence to: Jane E. Aubin, Department of Molecular and Medical Genetics, Faculty of Medicine, Rm. 6230, Medical Sciences Bldg., 1 King's College Circle, Toronto, Ont., M5S 1A8, Canada. E-mail: jane.aubin@utoronto.ca

Received 14 May 2003; Accepted 14 May 2003

DOI 10.1002/jcb.10596

The bone nodule assay has contributed to increased understanding of osteoblast differentiation [Nefussi et al., 1985; Bellows and Aubin, 1989; Rodan and Noda, 1991; Onyia et al., 1999]. In the RC and related models, expression of proliferation-associated (e.g., *c-fos*) and osteoblast-associated genes (e.g., type I collagen (COLLI), alkaline phosphatase (ALP), osteopontin (OPN), osteocalcin (OCN), bone sialoprotein (BSP)), are asynchronously upregulated, acquired, and/or lost as progenitor cells proliferate and differentiate and matrix matures and mineralizes [Owen et al., 1990; Rodan and Noda, 1991; Yao et al., 1994]. Together, the gene expression data support differentiation stages or a hierarchical relationship between more primitive versus more mature cells within the lineage [Lian and Stein, 1995; Aubin, 1998].

In spite of these advances, the lack of suitable markers to identify the most primitive osteoprogenitors has made their purification difficult, although some attempts to study lineage progression and to enrich for CFU-O have been made [Falla et al., 1993; Long et al., 1995; Chen et al., 1997; Zohar et al., 1997; Reyes and Verfaillie, 2001]. For example, antibodies (STRO-1, HOP-26) have been developed against adult human BM cells that aid in identification of early progenitor cells [Simmons and Torok-Storb, 1991; Gronthos et al., 1994; Joyner et al., 1997]. Sorting based on expression profiles of osteoblast-associated molecules, such as ALP, has enriched CFU-O in both rat BM stromal cell cultures [Herbertson and Aubin, 1997] and RC cell cultures [Turksen and Aubin, 1991]. In the latter study, the data also indicated that some CFU-O undergo default differentiation in culture while others require an inducing agent, such as dexamethasone (dex). Based on the presence or absence of ALP, those requiring dex are considered more primitive than those not requiring dex to differentiate in vitro [Turksen and Aubin, 1991]. Dex also appears to recruit or promote maturation of more primitive human osteoprogenitors [Stewart et al., 1999; Walsh et al., 2000, 2001]. Dual-color sorting based on STRO-1 and ALP of human BM stromal cells [Stewart et al., 1999; Walsh et al., 2000, 2001] and cells derived from human trabecular bone [Gronthos et al., 1999] has provided further evidence for a lineage hierarchy in which STRO-1^+/ALP^- osteoprogenitors progress to preosteoblasts (+/+) and osteoblasts (−/+) prior to a loss of expression of known osteoblast markers [Gronthos et al., 1999].

Many studies to date have relied on differences in marker expression, rather than functional outcome (i.e., capacity to form a bone nodule), to determine osteoprogenitor presence and differentiation or maturational status. To re-address the requirement of early bone nodule-forming osteoprogenitor cells for dex, to examine their differentiation status and marker expression, and to attempt to achieve more robust enrichment than has been achieved to date, we used dual color sorting with two known osteoblast-associated markers. Although discrepant and contradictory data exist on the differentiation stage-specific manner of parathyroid hormone/parathyroid hormone-related protein receptor (PTH1R) expression [Rouleau et al., 1988; Lee et al., 1993], reviewed [Aubin and Heersche, 2001], most data suggest that PTH1R is expressed at low levels relatively early in the differentiation cascade, with increasing expression as osteoblasts mature [Rodan and Noda, 1991; Liu et al., 2003], reviewed [Aubin and Heersche, 2001]. Based on its relatively restricted expression, and the view that it is regulated in a differentiation stage-specific manner, we reasoned that PTH1R might serve as a useful marker when paired with ALP, a relatively early marker of differentiating osteoblast precursors that increases then decreases as mineralization progresses.

By coupling gene expression and dex responsiveness, we report a surprising heterogeneity in the range of osteoprogenitors capable of forming bone nodules in vitro and evidence for both cell autonomous and non-autonomous differentiation of CFU-O.

MATERIALS AND METHODS

Reagents

Medium (α-minimum essential medium (αMEM)), phosphate-buffered saline (PBS), and citrate-buffered saline were purchased from the Tissue Culture Media Preparation core at the University of Toronto (Toronto, Ont.). Fetal bovine serum (FBS) was purchased from CanSera (Toronto, Ont.), and antibiotics were as follows: penicillin G (Sigma Chemical Co., St. Louis, MO), and gentamycin sulfate and fungizone from GibcoBRL, Burlington, ON. Trypsin was obtained from GibcoBRL. Ascorbic acid was obtained from Fisher Scientific, Hampton, NH,

and β-glycerophosphate (βGP), rat synthetic parathyroid hormone (PTH) (1–34), dex, and anhydrous ethyl alcohol were purchased from Sigma.

Cell Culture

RC cells. Fetal RC cells were obtained by sequential enzymatic digestion of calvariae from 21-day-old fetuses as previously described [Bellows et al., 1986]. Cells recovered from the last four digest steps (pop II-V) were plated separately in T-75 flasks containing αMEM, 15% heat-inactivated FBS, and antibiotics: 0.1 mg/ml penicillin G; 50 μg/ml gentamycin sulfate; 0.25 μg/ml fungizone. After 24 h, the cell populations were washed with PBS to remove debris and the adherent cells were collected with 0.2% trypsin in citrate-buffered saline. The viable cells were then pooled, resuspended in standard medium (10% FBS) as described above, and an aliquot counted with a hemocytometer. Experiments were performed with either the primary RC cells (collected 24 h after digest) or secondary RC cells that had been replated at $\sim 10^6$ cells/100-mm dish 24 h after the digest and allowed to grow for 3–4 days in standard medium. Medium was replenished every 2 days and cells were incubated at 37°C in a 5% CO_2 humidified atmosphere.

ROS 17/2.8 cells. ROS 17/2.8 cells (kindly provided by Dr. G. Rodan, Merck, West Point, PA) were maintained in αMEM, supplemented with 10% FBS and antibiotics (as above) in a humidified atmosphere with 5% CO_2 at 37°C. Medium was changed every other day and the cells grown in T-75 flasks were allowed to reach confluence either with or without the addition of dex (10^{-8} M) and ascorbic acid (50 μg/ml).

Flow Cytometry

Cell surface analysis. Cells were trypsinized as above, resuspended in ice cold Hanks-buffered salt solution containing 2% FBS (HF) and incubated at $\leq 10^7$ cells/ml for 45 min at 4°C using the appropriate dilutions of primary antibodies for ALP and PTH1R. The mouse monoclonal antibody RMB211.13 recognizing rat bone/liver/kidney ALP [Turksen and Aubin, 1991] was used at a 1:600 dilution in HF. A rabbit polyclonal antibody against PTH1R, purified via peptide affinity chromatography, was purchased from Covance Research Products, Inc., (Princeton, NJ). It (rat pep IV) was generated from a sequence in the first extracellular loop region of the rat PTH1R (CTLDESARLTEEELH) and was used at 1:50 or 1:100 dilution depending on the lot. Cells were washed twice in HF, incubated for 45 min at 4°C with fluorescein (FITC)-conjugated donkey anti-mouse IgG at 1:200 (H + L) and *R*-phycoerythrin (PE)-conjugated AffiniPure F(ab′)$_2$ fragment donkey anti-rabbit IgG (H + L) at 1:100 or 1:200 (Jackson ImmunoResearch Laboratories, Inc., (West Grove, PA), washed twice in HF, and resuspended in HF with 1 μg/ml 7-AAD (Molecular Probes Inc., Eugene, OR) for bulk sorting with EPICS ELITE (Beckman Coulter, Inc., Fullerton, CA) or single cell sorting with MoFlow® fluorescence activated cell sorting (FACS) (Cytomation, Fort Collins, CO), capable of sorting four subsets simultaneously with purity >99.5%. The 488 nm argon ion laser was used to excite samples, with emission being measured using appropriate band pass filters. Cells were passed through a 70 μm nylon cell strainer (Becton Dickinson, Franklin Lakes, NJ) prior to analysis to remove clumps. Viable cells (7-AAD$^-$) were collected in 4 ml tubes containing medium (15% FBS) or were sorted directly into 96-well plates containing 150 μl standard medium. Negative controls were employed with secondary antibodies alone. Due to a lack of high PTH1R expression in the RC population, compensation was set by using ROS 17/2.8 cells grown for 4–5 days with 10^{-8} M dex and 50 μg/ml ascorbic acid, as these conditions resulted in a high induction of PTH1R.

The sorted cell populations (viable/sort or ALP$^-$PTH1R$^-$, ALP$^-$PTH1R$^+$, ALP$^+$PTH1R$^-$, ALP$^+$PTH1R$^+$) were collected on ice and plated at densities ranging from 250 to 15,000 cells/well in 24-well plates (n = 6) in standard medium for the CFU-O assay. After 24 h, medium was changed to αMEM with 10% FBS, antibiotics, 50 μg/ml ascorbic acid, 10 mM βGP, and either vehicle control (0.11% ethanol; n = 3) or 10^{-8} M dex (n = 3). Cultures were maintained for 11–21 days prior to staining. The single cells sorted directly into 96-well plates from the four fractions and the control (viable/sort) were treated with either vehicle or dex for 32 days before von Kossa and ALP staining.

Immunolabeling

Immunolabeling of RC cultures was done as described previously [Liu et al., 1994]. Briefly, cultures were rinsed with PBS and fixed with

3.7% formaldehyde in PBS. Dishes were incubated for 45 min at 37°C with appropriate dilutions of primary antibodies in PBS (RBM211.13 at 1:600 purified ascites fluids, rat pep IV at 1:50 or 1:100) with 3% bovine serum albumin (BSA). Nodules were rinsed with PBS and then incubated for 30 min at room temperature with FITC-conjugated α-mouse IgG (1:200) and PE-conjugated $F(ab')_2$ α-rabbit IgG (1:200) prior to final rinse and mounting with Immuno Fluore Mounting Medium (ICN Biomedicals, Inc., Aurora, OH). Under the same conditions as specific labeling, controls with 3% BSA and secondary antibodies gave a weak fluorescent signal.

Quantification of Nodule Number and Area

Mineralized bone nodules were identified by double labeling for mineral (von Kossa stain) and ALP as described [Aubin, 1999]. The number of bone nodules was determined by manual counting on a microscope, alternatively dishes were scanned on a flatbed scanner (AGFA) with the number of bone nodules and area determined by image analysis with Image-Pro® Plus software (Media Cybernetic, L.P., Silver Spring, MD).

Statistical Analysis

Statistical assessment of the data included the calculation of 95% confidence intervals for sorted single cell studies, linear regression on standard density cultures, and the standard deviation of nodule numbers for all densities tested (triplicate samples). Results of statistical tests are as indicated in each figure and the table.

RESULTS

ALP and PTH1R Expression by Immunocytochemistry

During differentiation, RC cells differentially express various bone-related markers. We immunolocalized two early markers, ALP and PTH1R, in forming bone nodules and internodular cells. As expected, ALP was localized to the plasma membrane and highly expressed on cells associated with nascent bone nodules, while internodular cells had lower or undetectable expression levels. Some cells associated with nascent nodules, as well as cells in close proximity to the nodules, labeled for both ALP and PTH1R. Consistent with flow cytometry data (see below), fewer cells labeled detectably with PTH1R than with ALP (Fig. 1).

Fractionation of RC Cells Based Upon Cell Surface Expression of ALP and PTH1R

Immunocytochemistry suggested that ALP and PTH1R expression profiles might serve as useful developmental markers upon which to fractionate RC populations. Labeling conditions for ALP and PTH1R and flow cytometer settings for FACS analysis were first established with the ROS17/2.8 cell line grown with and without dex, which upregulates ALP and PTH1R expression (Fig. 2) [Rodan et al., 1984; Majeska et al., 1985; Onyia et al., 1999]. When RC cells were similarly labeled, four populations with different ALP and PTH1R expression profiles were observed. Although absolute numbers varied between triplicate experiments, trends were consistent with $53.8 \pm 18.2\%$ (39.2–74.2%) of RC cells found in the ALP^-PTH1R^- population, $3.2 \pm 3.2\%$ (1.1–6.9%) found in the ALP^-PTH1R^+ population, $33.3 \pm 15.6\%$ (21.7–51.1%) found in the ALP^+PTH1R^- population, and $9.7 \pm 7.7\%$ (2.7–17.9%) found in the ALP^+PTH1R^+ population.

CFU-O Reside in all Sorted Fractions but the Requirement for and Responsiveness to Dex Varies

We next determined in which fraction bone nodule-forming CFU-O cells reside and calculated their frequency across fractions. Fractionated populations were compared to two control populations: unlabeled and unsorted cells (viable/unsort) and labeled cells passed through the sorter but gated only on viability (viable/sort). Strikingly, CFU-O were found in all four fractions under control (vehicle) conditions although the number of nodules formed and the total mineralized area varied from fraction to fraction (Fig. 3). In vehicle, there was an average fold increase of 20.3 ± 2.9 CFU-O in the ALP^+PTH1R^- and ALP^+PTH1R^+ fractions compared to the viable/sort control, but the increase varied inversely with seeding density, i.e., from eightfold to tenfold at 12,000 cells/well versus 44-fold at 5,000 cells/well. Smaller differences were seen between the ALP^-PTH1R^- and the ALP^-PTH1R^+ populations versus the control population.

To examine the requirement for dex to elicit differentiation in each fraction and to examine whether CFU-O differentiation is cell autono-

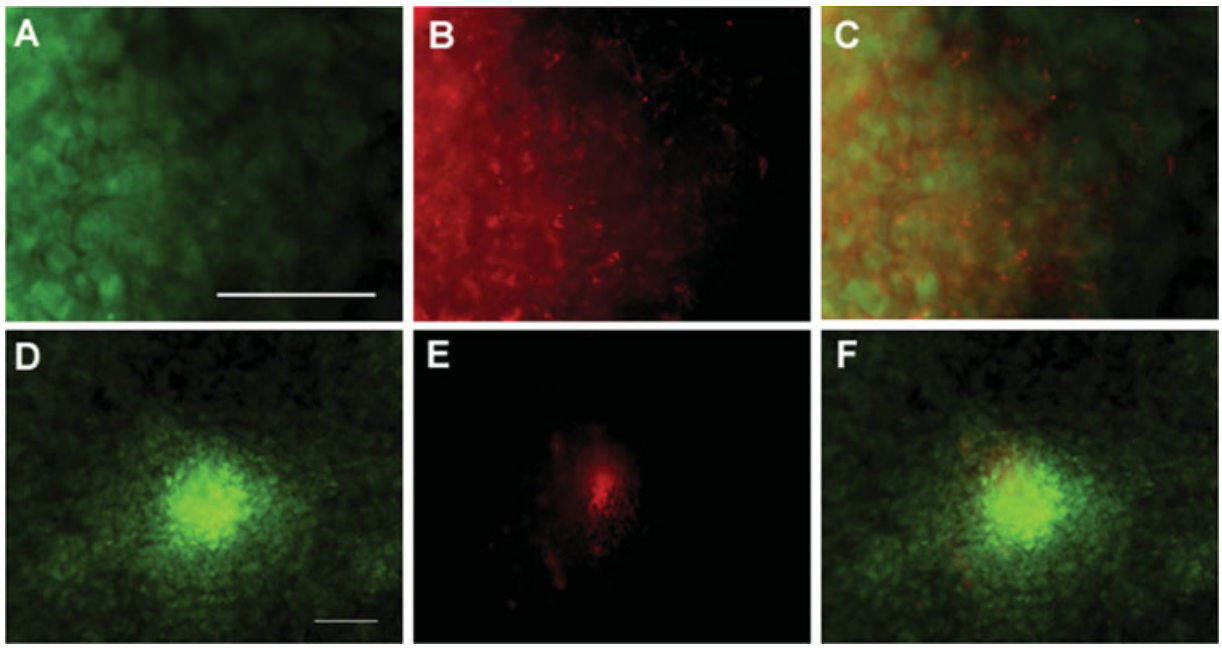

Fig. 1. Cells within nascent bone nodules express parathyroid hormone/parathyroid hormone-related protein receptor (PTH1R) and high alkaline phosphatase (ALP) levels on the cell surface; internodular cells do not express detectable PTH1R although some express ALP at lower levels. View of nodule and surrounding cells shown magnified 40× (**A**–**C**) or 16× (**D**–**F**) with fluorescent markers ALP–FITC (A, D), PTH1R–*R*-phycoerythrin (PE) (B, E), and merged images of ALP and PTH1R (C, F); 100 μm bar included for reference.

mous, cells were seeded at different densities. Viable/sort control cells were only half as responsive to dex as their viable/unsort counterparts, a result which was similar to the reported loss of dex responsive cells in rat BM following sorting [Herbertson and Aubin, 1997]. In all four sorted fractions, the number of nodules formed was higher in dex-treated versus vehicle-treated cultures, but the most marked increase was observed in $ALP^{-}PTH1R^{-}$ and $ALP^{-}PTH1R^{+}$ fractions (Fig. 4). In these two fractions, dex stimulated the number of nodules formed from 5- to 60-fold depending on cell plating density. Dex was much less effective in stimulating nodule formation in the $ALP^{+}PTH1R^{-}$ and $ALP^{+}PTH1R^{+}$ populations. Notably, linear regression analysis suggested that nodule number was proportional to plating density ($P < 0.05$) for all fractions grown in dex, but not for the $ALP^{-}PTH1R^{+}$ fraction, while in vehicle, only the $ALP^{+}PTH1R^{+}$ fraction appeared to be linear by statistical criteria (Table I). These data suggest that there is a significant cell non-autonomous aspect to precursor differentiation in all but the double positive cell fraction.

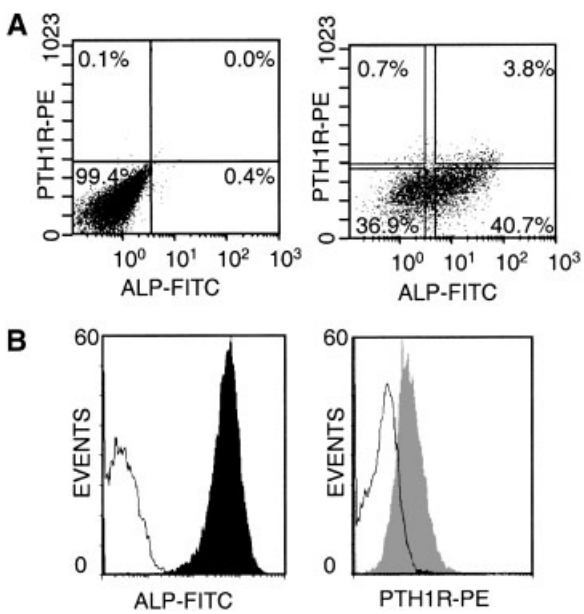

Fig. 2. Representative examples (of three experiments) from flow cytometry of rat calvaria (RC) and ROS 17/2.8 cells double-labeled for ALP and PTH1R. **A**: Plots of the negative control and the gates used to sort RC cell populations into four fractions ($ALP^{-}PTHR^{-}$, $ALP^{-}PTHR^{+}$, $ALP^{+}PTHR^{-}$, $ALP^{+}PTHR^{+}$). Only viable cells were sorted based on exclusion of 7-AAD. Control RC cells were either passed through the FACS machine without sorting (viable/sort) or were unlabeled and not passed through the sorter (viable/unsort). **B**: Flow cytometry compensation controls were set by using ROS 17/2.8 cells; overlaid histograms show the control versus labeled cells with ALP–FITC and PTHR–PE.

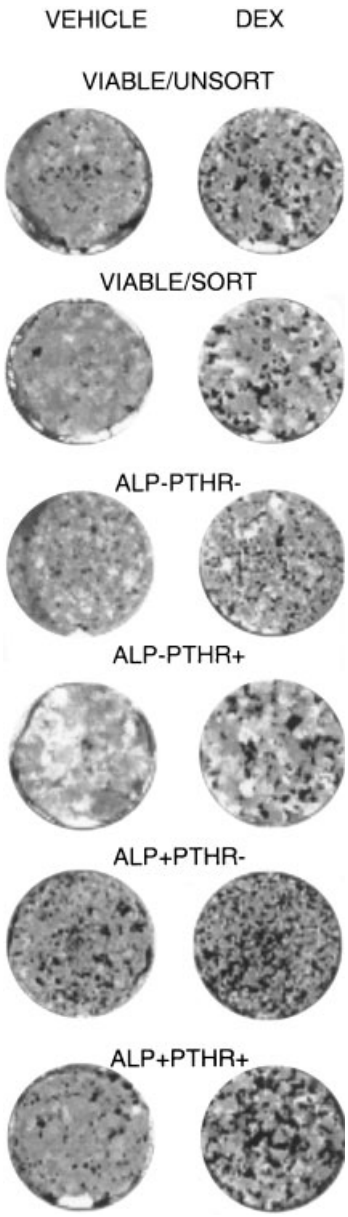

Fig. 3. All fractions sorted on the basis of ALP and PTH1R expression have osteogenic capacity (von Kossa and ALP stains). Dex enhanced colony forming unit-osteoblast (CFU-O) formation in all cases. Micrographs of representative examples (from triplicate wells of three independent experiments) are shown; cultures were initiated at 8,000 cells/well except for the $ALP^{-}PTHR^{+}$ fraction, which was seeded at 3,000 cells/well.

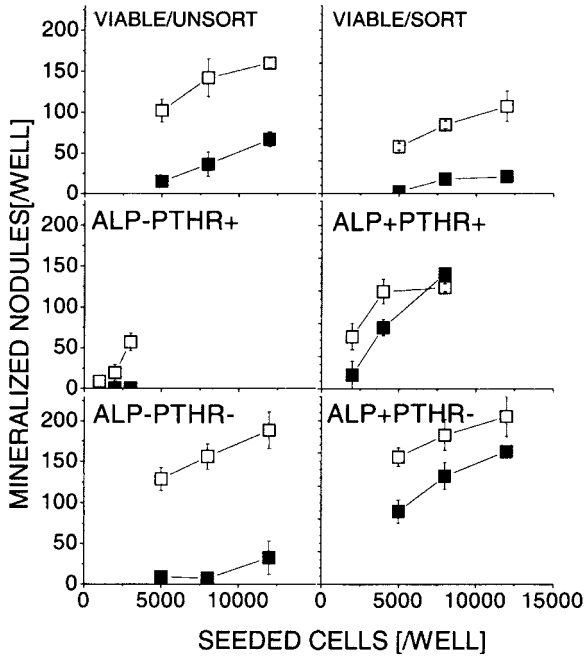

Fig. 4. Sorted fractions responded to dex with an increase in the number of CFU-O. The number of mineralized nodules is plotted against a range of plating densities for sorted cell fractions: $ALP^{-}PTH1R^{-}$, $ALP^{-}PTH1R^{+}$, $ALP^{+}PTH1R^{-}$, $ALP^{+}PTH1R^{+}$ grown in vehicle (■) or dex (□). Controls are in the top row; unstained and unsorted viable (based on trypan exclusion dye) cells (viable/unsort) and labeled cells sorted on viability alone ($7\text{-}AAD^{-}$; viable/sort). A representative experiment of three separate experiments is plotted and the mean number of nodules ± SD of triplicate wells per cell density is shown. The separation between nodule formation in each fraction assayed with dex and vehicle was significant ($P < 0.05$; Student's *t*-test, assuming unequal variances) except at the highest density of $ALP^{+}PTH1R^{-}$ and $ALP^{+}PTH1R^{+}$ populations or at the lowest density in $ALP^{-}PTH1R^{+}$ population.

Dex increased the frequency of osteoprogenitors in all fractions (calculated from the linear regression at non-clonal densities) with 1 in 93 ± 4, 52 ± 3, and 43 ± 2 cells functionally reading out as a CFU-O in the viable/sort, $ALP^{-}PTH1R^{-}$, and $ALP^{+}PTH1R^{-}$ fractions, respectively (Table I). The greatest increases were observed in the control and double negative fractions. Analysis of the $ALP^{+}PTH1R^{+}$ fraction was complicated by merging of mineralized nodules at high density, causing the curve to plateau (Fig. 4). The linear trend before saturation suggests the frequency of osteoprogenitors in the $ALP^{+}PTH1R^{+}$ fraction is approximately 1 in 33 cells.

Total mineralized area covered by nodules, however, did not directly correspond to nodule number (Fig. 5). In vehicle, there was an average 51.6 ± 10.5-fold increase in total mineralized area in cultures of $ALP^{+}PTH1R^{-}$ cells versus control populations. While cell yields limited the number of $ALP^{+}PTH1R^{+}$ cells that could be plated, generally, at seeding densities greater than 5,000 cells/well, a greater total mineralized area formed in the $ALP^{+}PTH1R^{+}$ population compared to the $ALP^{+}PTH1R^{-}$ population

TABLE I. Summary of Linear Regression Through the Origin for Nodule Output Versus Initial Number of Cells Seeded

	Summary of linear fit					
	Vehicle			Dex		
Condition	R	*P*	Frequency[a]	R	*P*	Frequency[a]
Viable/unsort	0.99	0.13	~1 in 240	0.99	0.34	~1 in 75
Viable/sort	0.90	0.16	~1 in 580	0.99	0.05	1 in 93 ± 4
ALP^-PTH1R^-	0.51	0.50	~1 in 680	0.99	<0.01	1 in 52 ± 3
ALP^-PTH1R^+	0	<0.01	~1 in 3,700	0.95	0.12	~1 in 70
ALP^+PTH1R^-	0.99	0.08	~1 in 75	0.99	<0.01	1 in 43 ± 2
ALP^+PTH1R^+	0.99	0.01	1 in 57 ± 1	0.85	<0.01	~1 in 35

The correlation coefficient (R), significance (*P*) of the linear model, and frequency of nodule formation is listed for each condition treated with vehicle or dex. The null hypothesis tested was that there was no correlation between nodule output and cell density (i.e., the slope = 0).
[a]The predicted frequency of osteoprogenitors in the sorted cell population was calculated from the inverse of the resultant slope of the linear regression of mineralized nodules at high density seeding. The '~' indicates that the prediction is approximate and may not be accurate due to differences between the observed data and the linear model.

(i.e., 1.8 ± 0.3-fold at 8,000 cells/well). Dex increased total mineralized area compared to that seen in vehicle in all populations. However, although similar nodule numbers were found after dex stimulation in the ALP^-PTH1R^-, ALP^+PTH1R^-, and ALP^+PTH1R^+ cell fractions (~1.5- to 3-fold over viable/sort), mineralized area covered by nodules was lower (0.7 ± 0.2) in the ALP^-PTH1R^- population but higher (2.5 ± 0.6 and 3.6 ± 0.5, respectively) in the ALP^+PTH1R^- and ALP^+PTH1R^+ populations compared to control.

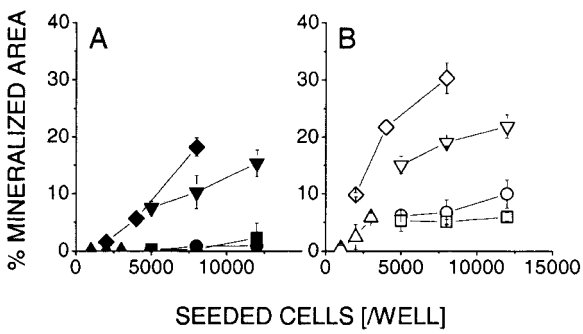

Fig. 5. Similar numbers of CFU-O yield different total mineralized nodule areas in different fractions. Fractions were grown continuously with vehicle (**A**, solid symbols) or dex (**B**, open symbols); results are shown for viable/sort (●), ALP^-PTHR^- (■), ALP^-PTHR^+ (▲), ALP^+PTHR^- (▼), and ALP^+PTHR^+ (◆) populations. A representative experiment (corresponds to Fig. 4) is plotted and the percentage of well surface area that was covered by mineralized matrix ± SD of triplicate wells per cell density is shown. The differences between the viable sort and the ALP^+PTH1R^- or ALP^+PTH1R^+ populations were significant in a pair-wise comparison of seeding density ($P < 0.05$; Student's *t*-test, assuming unequal variances).

Clonal Analysis of CFU-F and CFU-O

To assess clonal growth and differentiation, single viable cells of each sorted or unsorted population were seeded in 96-well plates. The plating efficiency (calculated as the percent of wells with adherent cells) was similar (60–90%) in all fractions except the ALP^-PTH1R^+ fraction, which was significantly lower (40%) than the viable/sort, ALP^-PTH1R^- and ALP^+-$PTHR^-$ populations (Fig. 6A). There was no significant difference in the number of CFU-F (fibroblast) colonies that formed in vehicle versus dex (Fig. 6B) nor was a difference seen in the distribution of colony sizes (data not shown) in any of the sorted fractions. In all fractions, a proportion of larger colonies (those that had grown for more than five population doublings) were ALP^+ (45–70% in vehicle), a number increased in the presence of dex but not significantly except in the ALP^-PTH1R^- fraction (Fig. 6C). However, CFU-O were detected at low frequency only in the ALP^-PTH1R^- fraction plated in either vehicle or dex, and in the viable/sort population in dex (Fig. 6D).

DISCUSSION

In this paper, we used dual-color FACS to fractionate RC cells into four subpopulations based on their surface phenotype ALP^-PTH1R^-, ALP^-PTH1R^+, ALP^+PTH1R^-, ALP^+PTH1R^+ and steroid response to interrogate developmental status. CFU-O capable of bone nodule formation were detectable in all fractions, suggesting that they do not represent

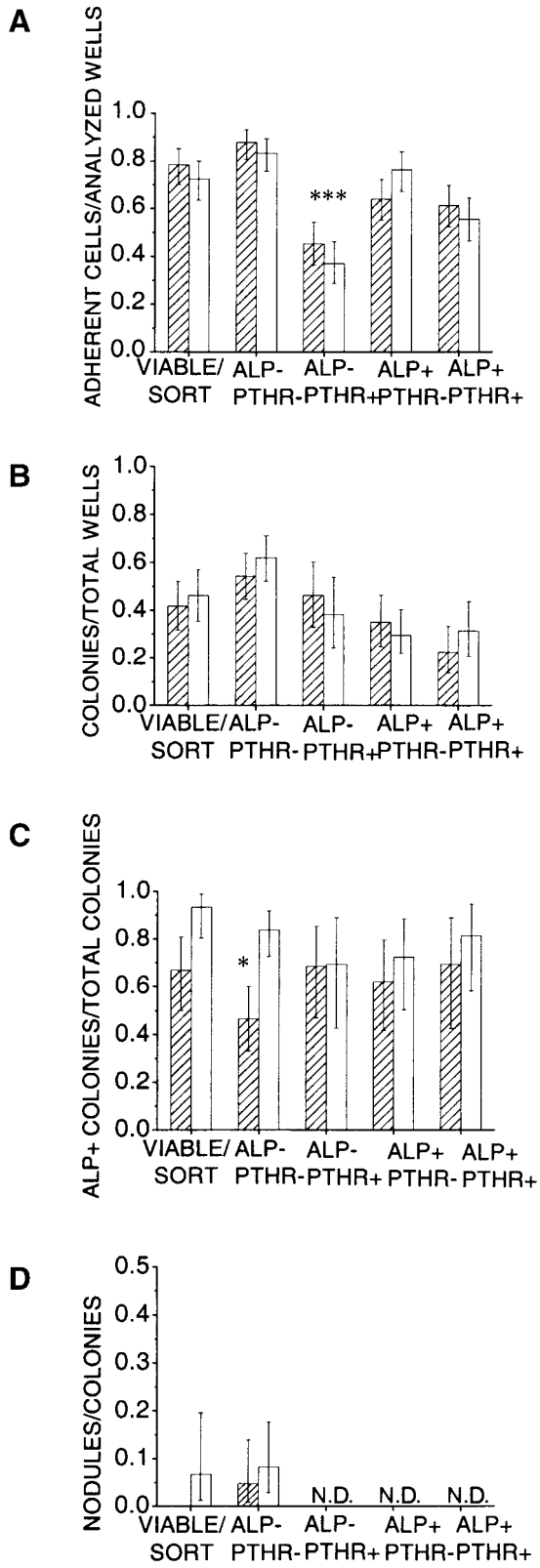

a single initiating progenitor type and that cells traditionally thought lacking in significant proliferative capacity may form nodules in vitro under some conditions. In agreement with our previous studies [Turksen and Aubin, 1991; Herbertson and Aubin, 1997], we also found that the majority of CFU-O with intrinsic capacity for differentiation are within the ALP^+ fraction, with or without PTH1R expression, and that the majority of dex requiring CFU-O are within the ALP^- fractions. In addition, however, we found that the only CFU-O with single cell autonomous osteogenic differentiation capacity are within the ALP^-PTH1R^- fraction, and that their differentiation appears to be under negative regulation by other cells in the RC population.

Our data on fractionated RC populations indicate multiple levels of regulation including the effects of inhibitory or stimulatory factors, and/or the effects of cell neighbors. Since osteoprogenitor proliferative potential is thought typically to decrease with cell differentiation or maturational status [Owen et al., 1990; de Pollak et al., 1997], we were intrigued to find bone nodule-forming cells present in all four-cell fractions, including the relatively mature ALP^+PTH1R^+ population. However, the ability to form a bone nodule, as well as the size of the nodule, was dependent upon both cell density and dex stimulation in the different fractions. These results suggest that not only developmental stage but also cell non-autonomous activities regulate progenitor differentiation in the RC model, a result not anticipated based on limiting dilution studies which showed linearity and a single limiting cell type, suggested to be the osteoprogenitor itself [Bellows and Aubin, 1989]. It is in keeping, however, with the cell non-autonomous behavior of osteoprogenitors in the rat BM stromal cell system [Aubin, 1999] and predicts that, in all osteogenesis models, a role for heterotypic cell interactions will need to

Fig. 6. Clonal analysis of double-labeled RC cells sorted individually into wells of 96-well plates and cultured for 32 days. The four populations (ALP^-PTH1R^-, ALP^-PTH1R^+, ALP^+PTH1R^-, ALP^+PTH1R^+) were compared to the viable/sort population in terms of plating efficiency (**A**), colony formation (**B**), ALP expression (**C**), and nodule formation capacity (**D**) of colonies in vehicle (hatched bars) or dex (open bars). Confidence intervals (95%) are shown; *** indicates significant difference between ALP^-PTH1R^+ and the other sorted fractions; * indicates significant difference between vehicle and dex assay conditions. N.D. indicates nodules were not detected.

be considered in drawing conclusions about developmental capacity.

Based on other studies in which CFU-O differentiation was followed at clonal densities [Malaval et al., 1999], it has also been suggested that immature progenitors may proliferate more extensively prior to matrix production and mineralization in comparison to cells more advanced in the lineage. Such a possibility might predict that the area covered by nodules and mineralized matrix produced by more immature progenitors would be larger than those produced by more mature cells in the lineage. However, we observed the opposite. One possibility for the apparent discrepancy remains that we have assessed the two-dimensional area of what are clearly three-dimensional structures, so that osteogenic potential is underestimated. Another possibility is that a particular cell density and/or matrix amount may be necessary to trigger terminal differentiation, which has been shown to be dependent on collagenous matrix deposition [Aronow et al., 1990; Owen et al., 1990; Stein and Lian, 1993], and this is easier to achieve amongst a more mature progenitor population. Finally, the ease of cell–cell communication via formation of gap-junctions may also be greater in more mature progenitor populations and may facilitate terminal differentiation and mineralization [Schiller et al., 2001].

Glucocorticoids are known to influence the proliferation and differentiation of cells of the osteoblast lineage, although effects are dependent on species, based on cellular context (in vivo or in vitro study), dose used, and the duration and time of exposure [Bellows et al., 1987; Murray et al., 1991; Cheng et al., 1994; Lian et al., 1997; Walsh et al., 2001]. We found that all four sorted RC cell fractions produced more nodules and displayed a larger mineralized area with dex, but the magnitude of the effect was fraction specific. The frequency of nodule formation also varied with plating cell density in both vehicle and dex treated cultures (Table I). Additionally, the frequencies of nodule formation predicted from the viable/sort and sorted fractions plated at high density were not observed in the experiments done at clonal density. Given the low predicted frequency, the nodule numbers observed in the $ALP^{-}PTH1R^{-}$ population plated clonally were particularly surprising. Notably, we found that dex treatment of single cells did not change plating or colony formation efficiency or colony size significantly, suggesting that changes in these parameters do not account for the observed differences, consistent with data in human stromal cell populations [Walsh et al., 2000]. Rather, this enrichment in the double negative population at the clonal level is suggestive of the presence of inhibitory cell populations and factors in this and the unsorted population. Soluble factors or stage-specific interactions between progenitors and their microenvironment have also been noted in other bone and non-bone cell populations [Ogiso et al., 1991; Roy and Verfaillie, 1997; Qu et al., 1999]. The lack of nodule formation in the $ALP^{+}PTH1R^{-}$ and $ALP^{+}PTH1R^{+}$ fractions may be due to a survival effect conferred through cell neighbors, but is less surprising as the plating efficiency of these populations is such that the analyzed cell numbers approach the threshold detection limit. Therefore, larger sample sizes are required to explore the clonal responses further. In addition, the data emphasize that caution is needed in drawing conclusions about absolute osteoprogenitor frequencies when cell non-autonomous interactions may enhance or mask intrinisic developmental potential.

The temporal and spatial expression of ALP and PTH1R in developing bone in vivo [Rodan and Noda, 1991; Kondo et al., 1997] and of differentiating osteoblasts in vitro [Owen et al., 1990; Bos et al., 1996; Nefussi et al., 1997; Siggelkow et al., 1999; Liu et al., 2003] has been studied in numerous experiments and most data support the concept that both ALP and PTH1R are progressively upregulated as osteoblasts mature. Consistent with this view, we found the cells associated with bone nodules to be $ALP^{+}PTH1R^{+}$ by immunocytochemistry (Fig. 1) and found an increase in the proportion of $ALP^{+}PTH1R^{+}$ cells in the RC population as nodules formed (data not shown). In addition, the double positive population did not emerge in cultures continuously treated with PTH, a condition known to suppress nodule formation (data not shown).

While all four fractions are clearly heterogeneous, it is probable that the double negative population is the most heterogeneous, in that it is expected to include uncommitted cells, cells of other lineages, and late stage cells of the osteoblast lineage. Osteoprogenitors expressing ALP appear to be primed to progress to functional osteoblasts, i.e., differentiation is a

default pathway in this population. In both ALP^+PTH1R^- and ALP^+PTH1R^+ populations, nodule yields in vehicle approached the maximal dex stimulated response. However, a greater mineralized area was found in the ALP^+PTH1R^+ population compared to the ALP^+PTH1R^- population. The level of differentiation, the loss of inhibitory factors, or the gain of stimulatory factors may distinguish the ALP^+PTH1R^- and ALP^+PTH1R^+ populations and explain this difference in mineralized area. Additionally, the average nodule size and total mineralized area in the double negative RC culture was lower than control and it exhibited the highest autonomy and CFU-O production at the clonal level. Thus, removal of inhibitory regulators, through the sorting of subpopulations, may contribute to the observed enrichment in this and other systems [Van Vlasselaer et al., 1994; Chen et al., 1997; Herbertson and Aubin, 1997; Zohar et al., 1997; Gronthos et al., 1999; Stewart et al., 1999]. In addition, the application and goal/end use of the sorted population would guide the sorting criteria further [i.e., is a cell population required that at low seeding densities (one cell) can progress to a bone nodule (double negative population) or is a cell population required that may have low proliferative and cloning efficiency but is capable of robust osteogenesis (double positive)]. The assay conditions employed support differentiation of CFU-O to bone nodules that lack detectable presence of other mesenchymal lineages, and that are morphologically and spatially distinct from fibroblastic colonies (CFU-F) that simultaneously form in the same cultures. However, we have not yet interrogated whether either progenitor type can differentiate into other mesenchymal lineages under appropriate assay conditions and further study may demonstrate differences in the proportions of cells capable of doing so in the fractionated populations.

In conclusion, we have presented evidence that the bone nodule-forming CFU-O within the RC cell population comprise heterogeneous progenitors with distinct surface expression profiles and distinct developmental capacities. Together, our fractionation and functional analysis data suggest a modified osteoblast developmental sequence (Fig. 7). Ranking the RC cell subpopulations in order of clonal capacity (i.e., immature cells capable of forming nodules at a single cell level), proportion of dex dependent cells (i.e., high dependence indicates

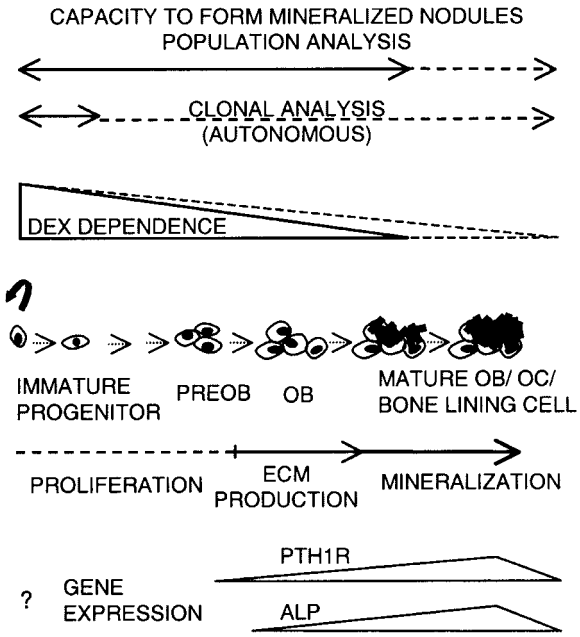

Fig. 7. A diagram illustrating the linear progression of cells from immature progenitor to functional osteoblast is shown with indications of maturity level, clonal capacity, dex dependence, and expression of ALP and PTH1R.

a population predominating in immature cells), and mineralized area (i.e., larger observable area indicates a more mature cell) results in the following gene progression: ALP^-PTH1R^- to ALP^-PTH1R^+ to ALP^+PTH1R^- to ALP^+-$PTH1R^+$. Although there are discrepancies, studies suggest that PTH1R is detectably expressed prior to ALP [Owen et al., 1990; Bos et al., 1996; Nefussi et al., 1997; Siggelkow et al., 1999; Liu et al., 2003], supporting this developmental sequence. However, such a sequence predicts biphasic expression profiles for PTH1R and ALP, an expression pattern that has not been reported to date and is, in fact, contradictory to what has usually been reported. These discrepancies suggest either that progenitor cells follow different developmental paths to maturity (i.e., a random transition from $-/-$ to $+/+$ through ALP^-PTH1R^+ or ALP^+PTH1R^-), a possibility consistent with our recent mathematical modeling of osteoblast development [Madras et al., 2002], or that cells with similar surface expression of these two markers are actually at different levels of differentiation. A confounding variable, not usually assessed, is that both cell autonomous and cell non-autonomous processes (i.e., inhibitory/stimulatory effects of neighboring cells

that are evident when functional output of the same population is assessed at different densities) influence osteoblast development in vitro. Use of additional surface or proliferation markers, and further analysis of CFU-O response to various factors may help resolve the questions that still surround the osteoprogenitor hierarchy and developmental sequence.

ACKNOWLEDGMENTS

The authors thank Cheryl Smith and Claude Cantin for excellent help with FACS sorting. KAP gratefully acknowledges student fellowship support from OGSST.

REFERENCES

Aronow MA, Gerstenfeld LC, Owen TA, Tassinari MS, Stein GS, Lian JB. 1990. Factors that promote progressive development of the osteoblast phenotype in cultured fetal rat calvaria cells. J Cell Physiol 143:213–221.

Aubin JE. 1998. Advances in the osteoblast lineage. Biochem Cell Biol 76:899–910.

Aubin JE. 1999. Osteoprogenitor cell frequency in rat bone marrow stromal populations: Role for heterotypic cell–cell interactions in osteoblast differentiation. J Cell Biochem 72:396–410.

Aubin JE, Heersche JNM. 2001. Cellular actions of parathyroid hormone on osteoblast and osteoclast differentiation: An update. In: Bilezikian J, Marcus R, Levine M, editors. The parathyroids. pp 199–211.

Bellows CG, Aubin JE. 1989. Determination of numbers of osteoprogenitors present in isolated fetal rat calvaria cells in vitro. Dev Biol 133:8–13.

Bellows CG, Aubin JE, Heersche JN, Antosz ME. 1986. Mineralized bone nodules formed in vitro from enzymatically released rat calvaria cell populations. Calcif Tissue Int 38:143–154.

Bellows CG, Aubin JE, Heersche JN. 1987. Physiological concentrations of glucocorticoids stimulate formation of bone nodules from isolated rat calvaria cells in vitro. Endocrinology 121:1985–1992.

Bellows CG, Ciaccia A, Heersche JN. 1998. Osteoprogenitor cells in cell populations derived from mouse and rat calvaria differ in their response to corticosterone, cortisol, and cortisone. Bone 23:119–125.

Bos MP, van der Meer JM, Feyen JH, Herrmann-Erlee MP. 1996. Expression of the parathyroid hormone receptor and correlation with other osteoblastic parameters in fetal rat osteoblasts. Calcif Tissue Int 58:95–100.

Chen JL, Hunt P, McElvain M, Black T, Kaufman S, Choi ES. 1997. Osteoblast precursor cells are found in CD34+ cells from human bone marrow. Stem Cells 15:368–377.

Cheng SL, Yang JW, Rifas L, Zhang SF, Avioli LV. 1994. Differentiation of human bone marrow osteogenic stromal cells in vitro: Induction of the osteoblast phenotype by dexamethasone. Endocrinology 134:277–286.

de Pollak C, Arnaud E, Renier D, Marie PJ. 1997. Age-related changes in bone formation, osteoblastic cell proliferation, and differentiation during postnatal osteogenesis in human calvaria. J Cell Biochem 64:128–139.

Falla N, Van Vlasselaer P, Bierkens J, Borremans B, Schoeters G, Van Gorp U. 1993. Characterization of a 5-fluorouracil-enriched osteoprogenitor population of the murine bone marrow. Blood 82:3580–3591.

Gerstenfeld LC, Chipman SD, Glowacki J, Lian JB. 1987. Expression of differentiated function by mineralizing cultures of chicken osteoblasts. Dev Biol 122: 49–60.

Gronthos S, Graves SE, Ohta S, Simmons PJ. 1994. The STRO-1+ fraction of adult human bone marrow contains the osteogenic precursors. Blood 84:4164–4173.

Gronthos S, Zannettino AC, Graves SE, Ohta S, Hay SJ, Simmons PJ. 1999. Differential cell surface expression of the STRO-1 and alkaline phosphatase antigens on discrete developmental stages in primary cultures of human bone cells. J Bone Miner Res 14:47–56.

Herbertson A, Aubin JE. 1997. Cell sorting enriches osteogenic populations in rat bone marrow stromal cell cultures. Bone 21:491–500.

Joyner CJ, Bennett A, Triffitt JT. 1997. Identification and enrichment of human osteoprogenitor cells by using differentiation stage-specific monoclonal antibodies. Bone 21:1–6.

Kondo H, Ohyama T, Ohya K, Kasugai S. 1997. Temporal changes of mRNA expression of matrix proteins and parathyroid hormone and parathyroid hormone-related protein (PTH/PTHrP) receptor in bone development. J Bone Miner Res 12:2089–2097.

Lee K, Deeds JD, Bond AT, Juppner H, Abou-Samra AB, Segre GV. 1993. In situ localization of PTH/PTHrP receptor mRNA in the bone of fetal and young rats. Bone 14:341–345.

Lian JB, Stein GS. 1995. Development of the osteoblast phenotype: Molecular mechanisms mediating osteoblast growth and differentiation. Iowa Orthop J 15:118–140.

Lian JB, Shalhoub V, Aslam F, Frenkel B, Green J, Hamrah M, Stein GS, Stein JL. 1997. Species-specific glucocorticoid and 1,25-dihydroxyvitamin D responsiveness in mouse MC3T3-E1 osteoblasts: Dexamethasone inhibits osteoblast differentiation and vitamin D downregulates osteocalcin gene expression. Endocrinology 138:2117–2127.

Liu F, Malaval L, Gupta AK, Aubin JE. 1994. Simultaneous detection of multiple bone-related mRNAs and protein expression during osteoblast differentiation: Polymerase chain reaction and immunocytochemical studies at the single cell level. Dev Biol 166:220–234.

Liu F, Malaval L, Aubin JE. 2003. Global amplification PCR reveals novel transitional stages in osteoprogenitor cells undergoing differentiation in vitro. J C Sci 116: 1787–1796.

Long MW, Robinson JA, Ashcraft EA, Mann KG. 1995. Regulation of human bone marrow-derived osteoprogenitor cells by osteogenic growth factors. J Clin Invest 95: 881–887.

Madras N, Gibbs AL, Zhou Y, Zandstra PW, Aubin JE. 2002. Modeling stem cell development by retrospective analysis of gene expression profiles in single progenitor-derived colonies. Stem Cells 20:230–240.

Majeska RJ, Nair BC, Rodan GA. 1985. Glucocorticoid regulation of alkaline phosphatase in the osteoblastic osteosarcoma cell line ROS 17/2.8. Endocrinology 116: 170–179.

Malaval L, Liu F, Roche P, Aubin JE. 1999. Kinetics of osteoprogenitor proliferation and osteoblast differentiation in vitro. J Cell Biochem 74:616–627.

Murray TM, Rao LG, Muzaffar SA. 1991. Dexamethasone-treated ROS 17/2.8 rat osteosarcoma cells are responsive to human carboxylterminal parathyroid hormone peptide hPTH (53–84): Stimulation of alkaline phosphatase. Calcif Tissue Int 49:120–123.

Nefussi JR, Boy-Lefevre ML, Boulekbache H, Forest N. 1985. Mineralization in vitro of matrix formed by osteoblasts isolated by collagenase digestion. Differentiation 29:160–168.

Nefussi JR, Brami G, Modrowski D, Oboeuf M, Forest N. 1997. Sequential expression of bone matrix proteins during rat calvaria osteoblast differentiation and bone nodule formation in vitro. J Histochem Cytochem 45: 493–503.

Nishida S, Endo N, Yamagiwa H, Tanizawa T, Takahashi HE. 1999. Number of osteoprogenitor cells in human bone marrow markedly decreases after skeletal maturation. J Bone Miner Metab 17:171–177.

Ogiso B, Hughes FJ, Melcher AH, McCulloch CA. 1991. Fibroblasts inhibit mineralised bone nodule formation by rat bone marrow stromal cells in vitro. J Cell Physiol 146:442–450.

Onyia JE, Hale LV, Miles RR, Cain RL, Tu Y, Hulman JF, Hock JM, Santerre RF. 1999. Molecular characterization of gene expression changes in ROS 17/2.8 cells cultured in diffusion chambers in vivo. Calcif Tissue Int 65:133–138.

Owen TA, Aronow M, Shalhoub V, Barone LM, Wilming L, Tassinari MS, Kennedy MB, Pockwinse S, Lian JB, Stein GS. 1990. Progressive development of the rat osteoblast phenotype in vitro: Reciprocal relationships in expression of genes associated with osteoblast proliferation and differentiation during formation of the bone extracellular matrix. J Cell Physiol 143:420–430.

Qu Q, Harkonen PL, Monkkonen J, Vaananen HK. 1999. Conditioned medium of estrogen-treated osteoblasts inhibits osteoclast maturation and function in vitro. Bone 25:211–215.

Reyes M, Verfaillie CM. 2001. Characterization of multipotent adult progenitor cells, a subpopulation of mesenchymal stem cells. Ann NY Acad Sci 938:231–233; discussion 233–235.

Rodan GA, Noda M. 1991. Gene expression in osteoblastic cells. Crit Rev Eukaryot Gene Expr 1:85–98.

Rodan SB, Fischer MK, Egan JJ, Epstein PM, Rodan GA. 1984. The effect of dexamethasone on parathyroid hormone stimulation of adenylate cyclase in ROS 17/2.8 cells. Endocrinology 115:951–958.

Rouleau MF, Mitchell J, Goltzman D. 1988. In vivo distribution of parathyroid hormone receptors in bone: Evidence that a predominant osseous target cell is not the mature osteoblast. Endocrinology 123:187–191.

Roy V, Verfaillie CM. 1997. Soluble factor(s) produced by adult bone marrow stroma inhibit in vitro proliferation and differentiation of fetal liver BFU-E by inducing apoptosis. J Clin Invest 100:912–920.

Schiller PC, D'Ippolito G, Balkan W, Roos BA, Howard GA. 2001. Gap-junctional communication is required for the maturation process of osteoblastic cells in culture. Bone 28:362–369.

Siggelkow H, Rebenstorff K, Kurre W, Niedhart C, Engel I, Schulz H, Atkinson MJ, Hufner M. 1999. Development of the osteoblast phenotype in primary human osteoblasts in culture: Comparison with rat calvarial cells in osteoblast differentiation. J Cell Biochem 75:22–35.

Simmons PJ, Torok-Storb B. 1991. Identification of stromal cell precursors in human bone marrow by a novel monoclonal antibody, STRO-1. Blood 78:55–62.

Stein GS, Lian JB. 1993. Molecular mechanisms mediating proliferation/differentiation interrelationships during progressive development of the osteoblast phenotype. Endocr Rev 14:424–442.

Stewart K, Walsh S, Screen J, Jefferiss CM, Chainey J, Jordan GR, Beresford JN. 1999. Further characterization of cells expressing STRO-1 in cultures of adult human bone marrow stromal cells. J Bone Miner Res 14:1345–1356.

Turksen K, Aubin JE. 1991. Positive and negative immunoselection for enrichment of two classes of osteoprogenitor cells. J Cell Biol 114:373–384.

Van Vlasselaer P, Falla N, Snoeck H, Mathieu E. 1994. Characterization and purification of osteogenic cells from murine bone marrow by two-color cell sorting using anti-Sca-1 monoclonal antibody and wheat germ agglutinin. Blood 84:753–763.

Walsh S, Jefferiss C, Stewart K, Jordan GR, Screen J, Beresford JN. 2000. Expression of the developmental markers STRO-1 and alkaline phosphatase in cultures of human marrow stromal cells: Regulation by fibroblast growth factor (FGF)-2 and relationship to the expression of FGF receptors 1–4. Bone 27:185–195.

Walsh S, Jordan GR, Jefferiss C, Stewart K, Beresford JN. 2001. High concentrations of dexamethasone suppress the proliferation but not the differentiation or further maturation of human osteoblast precursors in vitro: Relevance to glucocorticoid-induced osteoporosis. Rheumatology (Oxford) 40:74–83.

Yao KL, Todescan R, Jr., Sodek J. 1994. Temporal changes in matrix protein synthesis and mRNA expression during mineralized tissue formation by adult rat bone marrow cells in culture. J Bone Miner Res 9:231–240.

Zohar R, Sodek J, McCulloch CA. 1997. Characterization of stromal progenitor cells enriched by flow cytometry. Blood 90:3471–3481.